JOURNAL OF MATERIALS SCIENCE 26 (1991) 6507–6516

Chemical reactions between $YBa_2Cu_3O_{6+\delta}$ and potential hot-forging die materials

B. R. POWELL, R. L. BLOINK
Metallurgy Department, General Motors Research Laboratories, Warren, Michigan 48090, USA
R. A. WALDO
Analytical Chemistry Department, General Motors Research Laboratories, Warren, Michigan 48090, USA

A survey of the reactivity of $YBa_2Cu_3O_{6+\delta}$ with several oxide and non-oxide materials was conducted to identify die materials for use in hot-forging studies of $YBa_2Cu_3O_{6+\delta}$. Reactivity was determined at 850 and 950 °C. The nature and extent of chemical reactions were assessed by electron probe microanalysis. Barium zirconate and silicon carbide showed negligible chemical reaction with $YBa_2Cu_3O_{6+\delta}$. Magnesium oxide and zirconium dioxide did react, but the products appear to have inhibited further reactions. Other materials such as aluminium nitride, zirconium diboride, and boron carbide, showed extensive chemical reactions with $YBa_2Cu_3O_{6+\delta}$.

1. Introduction

The discovery of $YBa_2Cu_3O_{6+\delta}$ [1] resulted in a worldwide effort to understand superconductivity in this new class of materials and to develop these materials into superconducting devices. Unfortunately, success in applying these materials to new devices has been very limited, in part because of the detrimental effect of grain boundaries in both thin film and bulk ceramic superconductors. The grain boundaries lower the electrical current that the material can carry while in the superconducting state [2]. Consequently, attempts have been made to eliminate the grain boundaries in ceramic superconductors.

Whereas grain boundaries can be eliminated in thin-film superconductors by growing $YBa_2Cu_3O_{6+\delta}$ epitaxially on suitable substrates, this method is not feasible for bulk $YBa_2Cu_3O_{6+\delta}$. Instead, one approach has been the use of forming processes which are known to cause crystallite alignment during densification [3, 4]. Among these processes are hot pressing and hot forging in which powder compacts are heated to the densification temperature, and then subjected to external pressure. In hot pressing, the pressure promotes densification of the material, which already fills the die cavity. In hot forging, the material flows and fills the die cavity. In each case, the degree of crystallite alignment is increased, although the degree of alignment is higher in hot-forged materials than in hot-pressed materials.

Unfortunately, $YBa_2Cu_3O_{6+\delta}$ reacts readily with many of the materials that are used as hot-forging dies. For this reason, a study was undertaken to identify suitable die materials for hot forging of $YBa_2Cu_3O_{6+\delta}$.

2. Experimental procedure

Eleven ceramic materials were tested for chemical compatibility with $YBa_2Cu_3O_{6+\delta}$. The following ceramics were obtained from suppliers: aluminium nitride, aluminium oxide, boron carbide, boron nitride, boron nitride–titanium diboride, magnesium oxide, silicon carbide, zirconium diboride, and yttrium oxide–stabilized zirconium dioxide. Barium zirconate was synthesized in this laboratory and magnesium oxide–stabilized zirconium dioxide was cut from a hot-pressing die insert.

$YBa_2Cu_3O_{6+\delta}$ powder was prepared from a spray-dried aqueous solution of yttrium acetate, barium acetate, and copper nitrate [5]. Yttrium acetate was dissolved in distilled water by adding concentrated nitric acid. To this solution were added appropriate amounts of barium acetate and copper nitrate stock solutions to yield a Y:Ba:Cu atom ratio of 1:2:3. Spray drying consisted of atomizing the solution in a chamber of hot, swirling air. The dried and partially decomposed salts were carried in the air stream through the outlet of the chamber and collected in a cyclone filter. The inlet and outlet temperatures during spray drying were 180 and 90 °C, respectively. Spray drying yielded a solid product that was then calcined at 850 °C for 12 h in flowing hydrocarbon-free air. Chemical analysis of the calcined powder showed that the Y:Ba:Cu atom ratio was still 1.0:2.0:3.0. X-ray diffraction (XRD) analysis showed the powder to be single-phase $YBa_2Cu_3O_{6+\delta}$.

Samples of each material tested for compatibility were set in aluminium oxide crucibles and $YBa_2Cu_3O_{6+\delta}$ powder was placed on top of each. The crucibles were heated in a tube furnace with a fused silica muffle. Treatments at 850 °C for 4 h were to simulate hot-forging experiments. Treatments at 950 °C for 6 or 19 h were conducted to represent worst case scenarios for hot forging, and to screen materials for possible melt-processing experiments. After

0022–2461/91 $03.00 + .12

cooling, the specimens (reaction couples) were removed from the furnace and sectioned with a diamond wheel using oleum as a coolant. Samples were mounted in bakelite and polished in preparation for electron probe microanalysis (EPMA). EPMA was used to acquire distribution maps for elements of interest. In some cases, EPMA was also used to determine the quantitative chemical composition of selected areas.

3. Results and discussion

The nature and extent of chemical reaction between $YBa_2Cu_3O_{6+\delta}$ and each of the candidate materials is described below. In each case where EPMA results are shown, the figures are oriented so that $YBa_2Cu_3O_{6+\delta}$ side of the reaction couple is in the upper portion of the figure.

3.1. Barium zirconate

Barium zirconate has been identified as a product of the reaction between $YBa_2Cu_3O_{6+\delta}$ and zirconium dioxide [6, 7]. The compound was prepared for this study by reacting barium carbonate and zirconium dioxide powders at 1540 °C for 1 h in air. The barium zirconate powder was then pressed and sintered into a disc.

The reaction couple was treated at 950 °C for 19 h. EPMA results, shown in Fig. 1, indicate that no reaction interface forms and there is no wetting of the barium zirconate by $YBa_2Cu_3O_{6+\delta}$. Neither yttrium nor zirconium diffuse across the reaction couple, although trace amounts of copper are observed in the barium zirconate side of the reaction couple. Yttrium appears to be segregated in the $YBa_2Cu_3O_{6+\delta}$. Prior experience suggests that the yttrium-rich regions are Y_2BaCuO_5, but XRD analysis of the powder did not detect this or any other phases. Thus, barium zirconate shows significant promise for use in $YBa_2Cu_3O_{6+\delta}$ processing.

3.2. Silicon carbide

Silicon carbide shows considerable promise as a processing material for $YBa_2Cu_3O_{6+\delta}$. The reaction couple, following treatment at 850 °C for 4 h, is shown in Fig. 2. There is essentially no chemical reaction between silicon carbide and $YBa_2Cu_3O_{6+\delta}$, based on the silicon, yttrium, and barium maps. The carbon map, not shown, is inconclusive. There does not appear to be any wetting between the two materials. Furthermore, no segregation has occurred in the $YBa_2Cu_3O_{6+\delta}$; the copper map, which is not shown, is nearly identical to the barium map, which is shown in Fig. 2. The silicon map gives some indication of silicon presence in the $YBa_2Cu_3O_{6+\delta}$, but this may be an artefact due to the different background intensity for silicon in $YBa_2Cu_3O_{6+\delta}$, relative to its

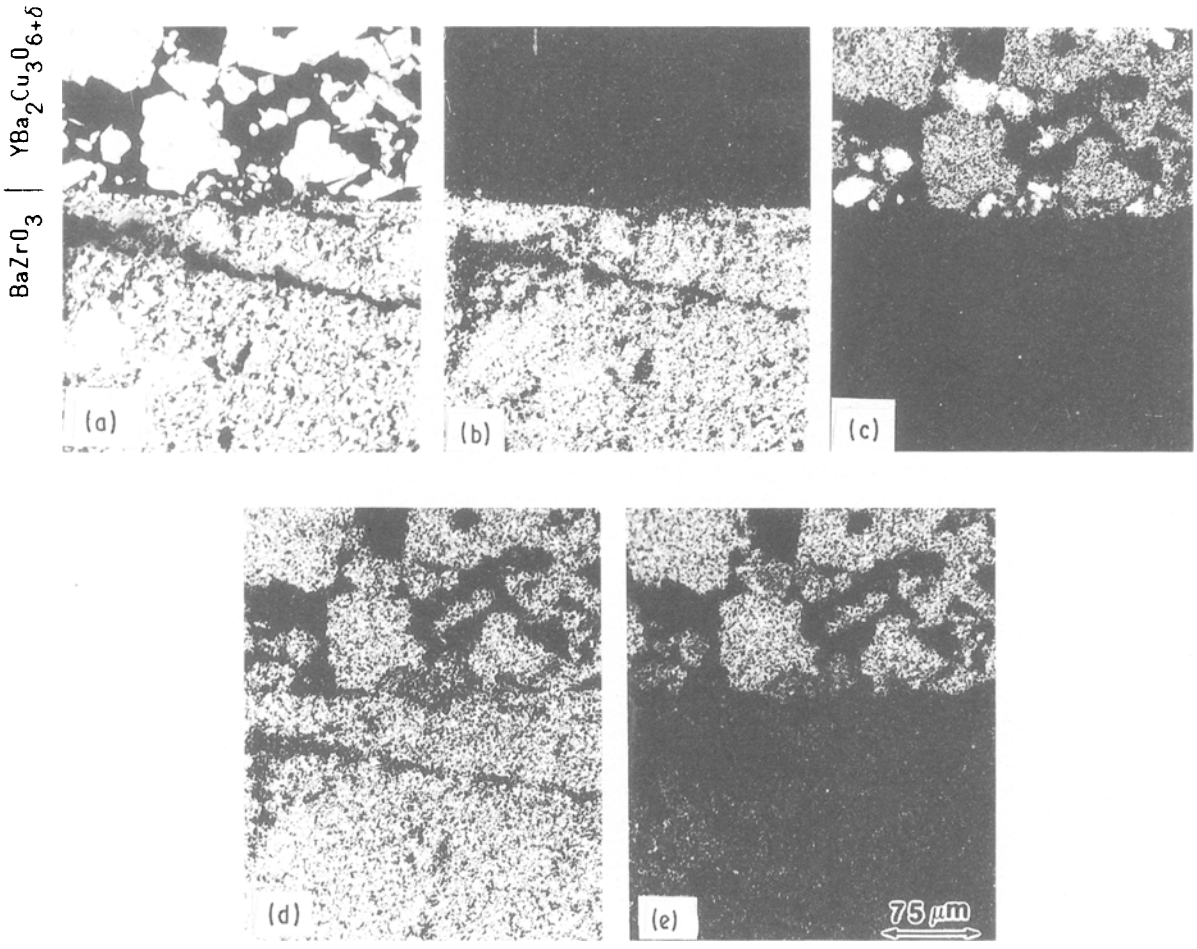

Figure 1 EPMA of the barium zirconate–$YBa_2Cu_3O_{6+\delta}$ reaction couple treated at 950 °C for 19 h. (a) Backscattered electron image, and elemental maps for (b) zirconium, (c) yttrium, (d) barium, and (e) copper.

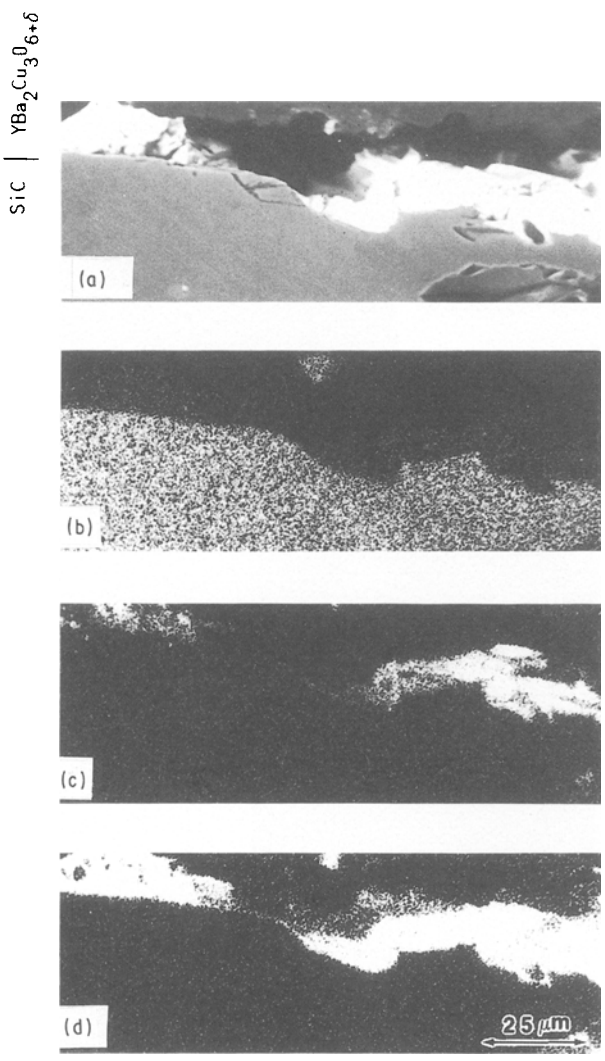

Figure 2 EPMA of the silicon carbide–$YBa_2Cu_3O_{6+\delta}$ reaction couple treated at 850 °C for 4 h. (a) Backscattered electron image, and elemental maps for (b) silicon, (c) yttrium, and (d) barium.

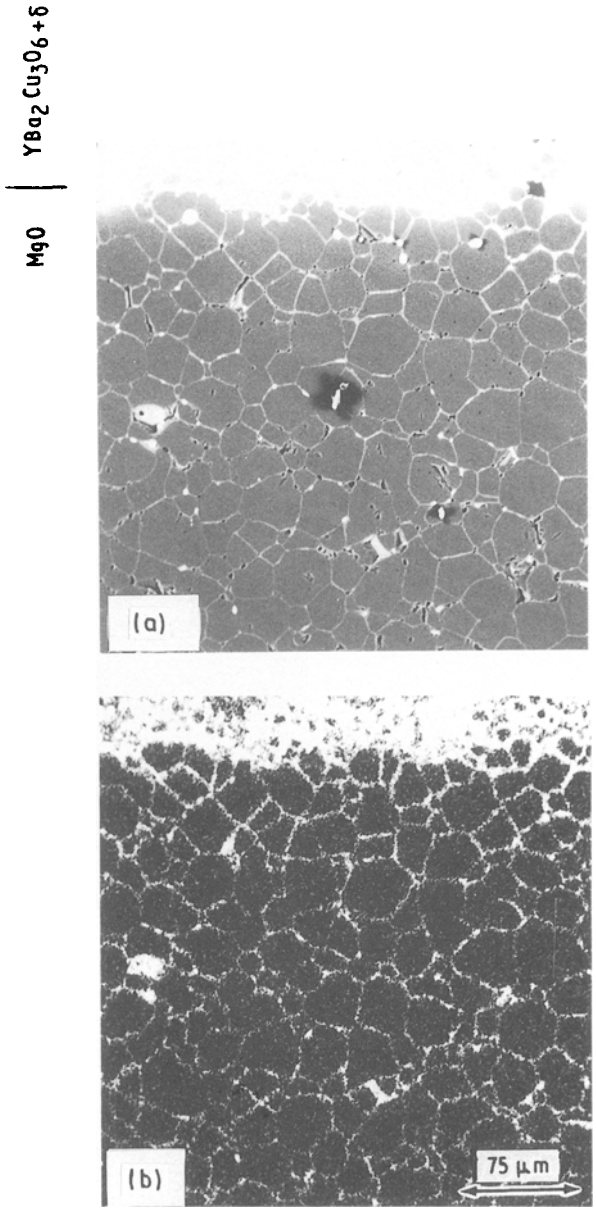

Figure 3 EPMA of the magnesium oxide–$YBa_2Cu_3O_{6+\delta}$ reaction couple treated at 950 °C for 19 h. (a) Backscattered electron image, and (b) the elemental map for copper.

background in silicon carbide or the mounting material. The results for the reaction couple treated at 950 °C for 19 h are the same.

3.3. Magnesium oxide

Magnesium oxide single crystals have been used as substrates for superconducting thin films [6, 8, 9]. As a single crystal, the only reported reaction is the formation of copper-rich precipitates at the interface. The polycrystalline specimen used in this work shows extensive reaction, essentially all of it occurring at the grain boundaries, see Fig. 3. In this sample, which was reacted at 950 °C for 19 h, copper oxide has diffused along, and effectively decorated, the magnesium oxide grain boundaries. Concerning the mechanism of this process, yttrium, barium, silicon, and calcium, were not detected in the grain boundaries. It is possible that magnesium oxide, pretreated with copper oxide, might be a suitable material for superconductor processing.

3.4. Zirconium dioxide

The reaction of zirconium dioxide with $YBa_2Cu_3O_{6+\delta}$ has been described previously [6, 7]. The reaction results in the formation of barium zirconate, copper oxide, and Y_2BaCuO_5. Two types of zirconium dioxide were evaluated in this study: partially stabilized (using yttrium oxide) and fully stabilized (using magnesium oxide). Both samples were reacted at 950 °C for 6 h instead of 19 h. It is not expected that reaction results were significantly altered by this change in time. The yttrium oxide-stabilized zirconia is shown in Fig. 4. It appears that barium has diffused into the zirconium dioxide leaving a barium-poor region in what was originally stoichiometric $YBa_2Cu_3O_{6+\delta}$. This region is also somewhat yttrium-poor. Sintering $YBa_2Cu_3O_{6+\delta}$ on discs of yttrium oxide-stabilized zirconia usually leaves the surface of the disc blackened indicating some diffusion of copper into it. The magnesium oxide-stabilized zirconium dioxide behaved similarly, see Fig. 5. In this sample, the barium zirconate layer has no magnesium in it, which suggests that the compound formed in the $YBa_2Cu_3O_{6+\delta}$ side of the reaction couple. A region of stoichiometric

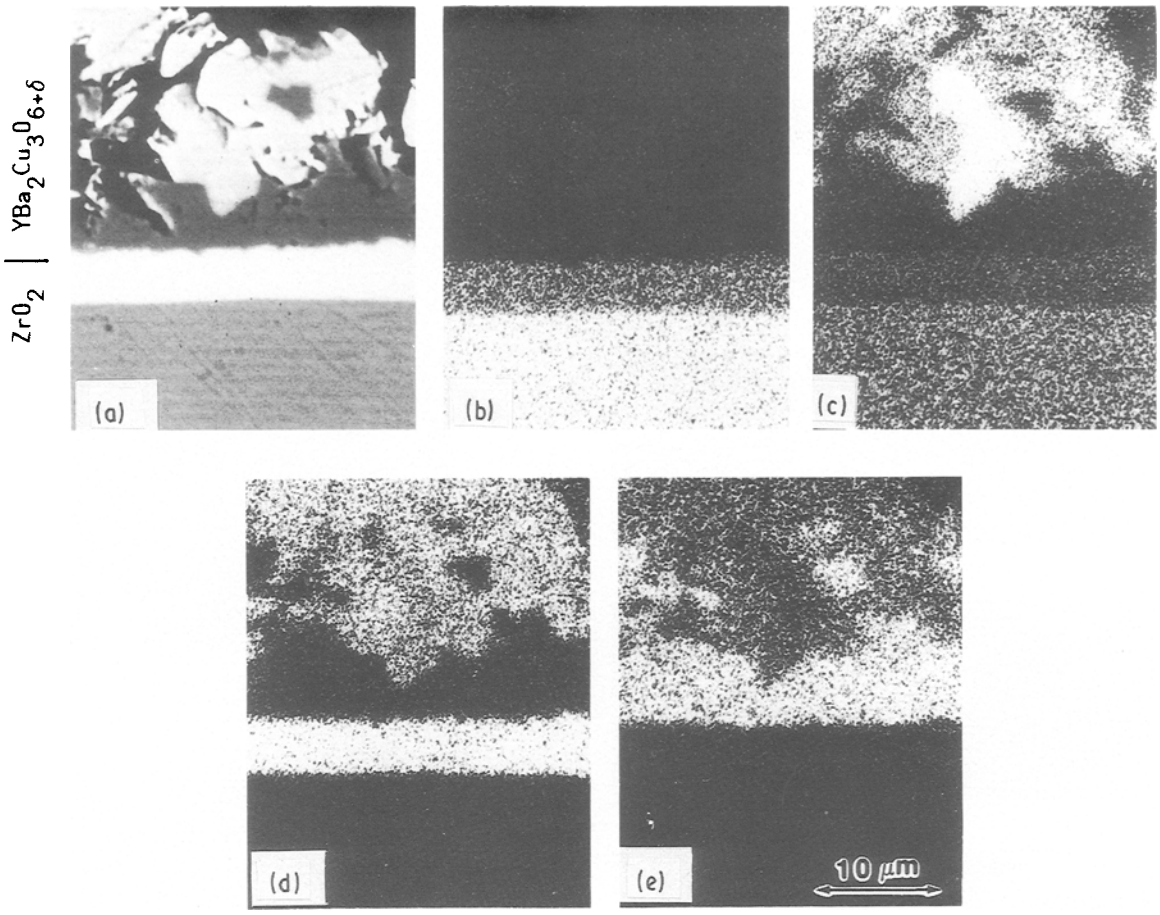

Figure 4 EPMA of the yttrium oxide-stabilized zirconium dioxide–$YBa_2Cu_3O_{6+\delta}$ reaction couple treated at 950 °C for 6 h. (a) Backscattered electron image, and elemental maps for (b) zirconium, (c) yttrium, (d) barium, and (e) copper.

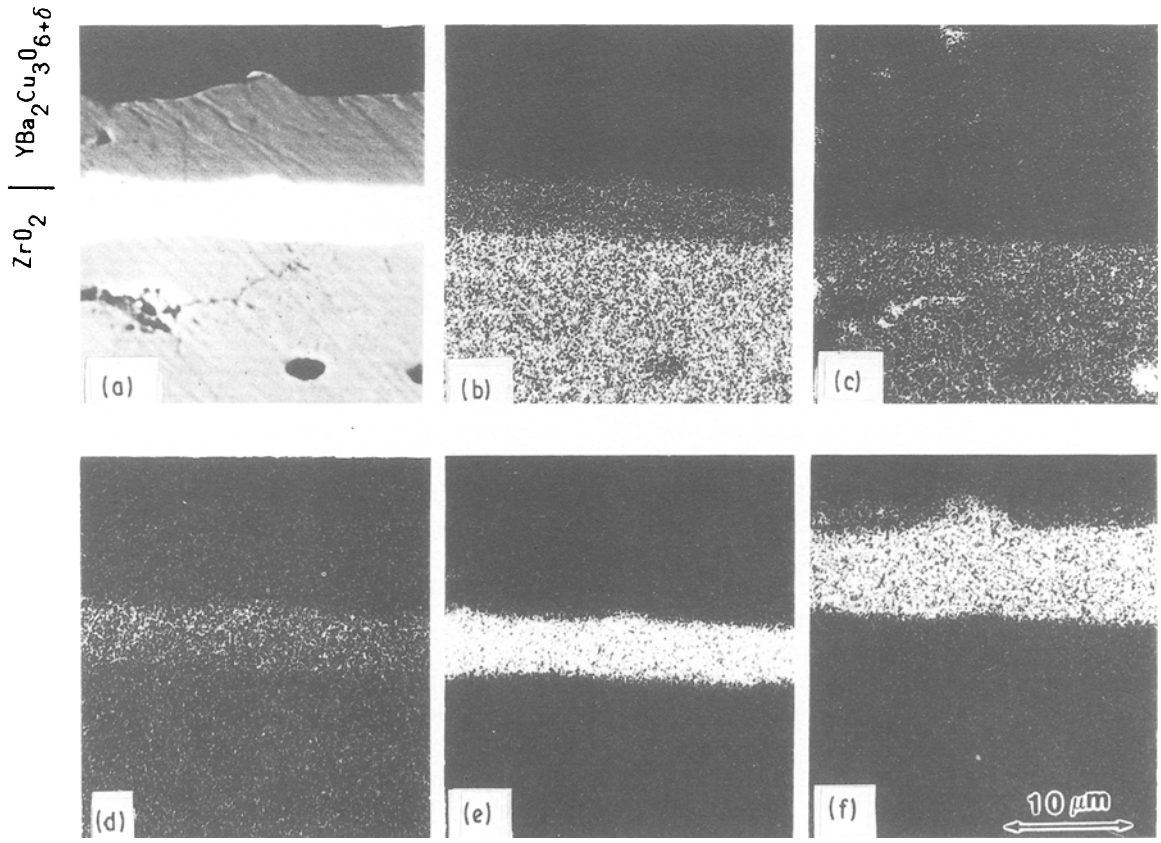

Figure 5 EPMA of the magnesium oxide-stabilized zirconium dioxide–$YBa_2Cu_3O_{6+\delta}$ reaction couple, treated at 950 °C for 6 h.(a) Backscattered electron image, and elemental maps for (b) zirconium, (c) magnesium, (d) yttrium, (e) barium, and (f) copper.

$YBa_2Cu_3O_{6+\delta}$ is not visible in the figure. Presumably, it was removed during sectioning.

A die made of magnesium oxide-stabilized zirconium dioxide was used successfully to hot forge $YBa_2Cu_3O_{6+\delta}$ samples. Discolouration of the die surfaces occurred, but the $YBa_2Cu_3O_{6+\delta}$ samples did not adhere to the die surface. Possibly the surfaces of the die components had been converted, over time, to barium zirconate which effectively prevents future reactions and adhesion. Given these considerations, magnesium oxide-stabilized zirconium dioxide should be a good die material for hot forging $YBa_2Cu_3O_{6+\delta}$.

3.5. Boron carbide

Thermal treatment of the boron carbide–$YBa_2Cu_3O_{6+\delta}$ couple at 950 °C for 19 h, caused extensive reaction as well as excessive grain growth in the $YBa_2Cu_3O_{6+\delta}$. Whereas boron did not diffuse extensively into the $YBa_2Cu_3O_{6+\delta}$, barium did diffuse into the boron carbide, see Fig. 6. Furthermore, metallic copper segregated at the reaction interface. The layer of copper was obvious, even to the naked eye. EPMA confirmed this and revealed a copper-poor region in the $YBa_2Cu_3O_{6+\delta}$ next to the copper-rich layer. The reaction couple treated at 850 °C for 4 h showed the same results, although the extent of grain growth and the degree of segregation of copper was less. Boron carbide is not suitable for die materials.

3.6. Aluminium nitride

The aluminium nitride–$YBa_2Cu_3O_{6+\delta}$ couple was treated at 950 °C for 19 h. The aluminium nitride acquired a copper colour as though copper had deposited on its surface. In areas where discrete particles of $YBa_2Cu_3O_{6+\delta}$ had rested during the heat treatment a copper-coloured ring appeared and the $YBa_2Cu_3O_{6+\delta}$ particles turned green, indicating a reduced copper oxide content in the $YBa_2Cu_3O_{6+\delta}$ and decomposition to Y_2BaCuO_5. EPMA indicated approximately 0.5% aluminium in the $YBa_2Cu_3O_{6+\delta}$ side of the reaction couple. Nitrogen also appears to have diffused throughout the superconductor although the intensity of the nitrogen signal in the nitrogen map, see Fig. 7, may be due to a high background intensity. The reaction zone containing elements from both reactants extends nearly to the top of the superconductor layer. The original $YBa_2Cu_3O_{6+\delta}$ regions were deficient in barium. Yttrium segregation at the free surface of the $YBa_2Cu_3O_{6+\delta}$ is also apparent, and is consistent with the visual observation of Y_2BaCuO_5. The extent of

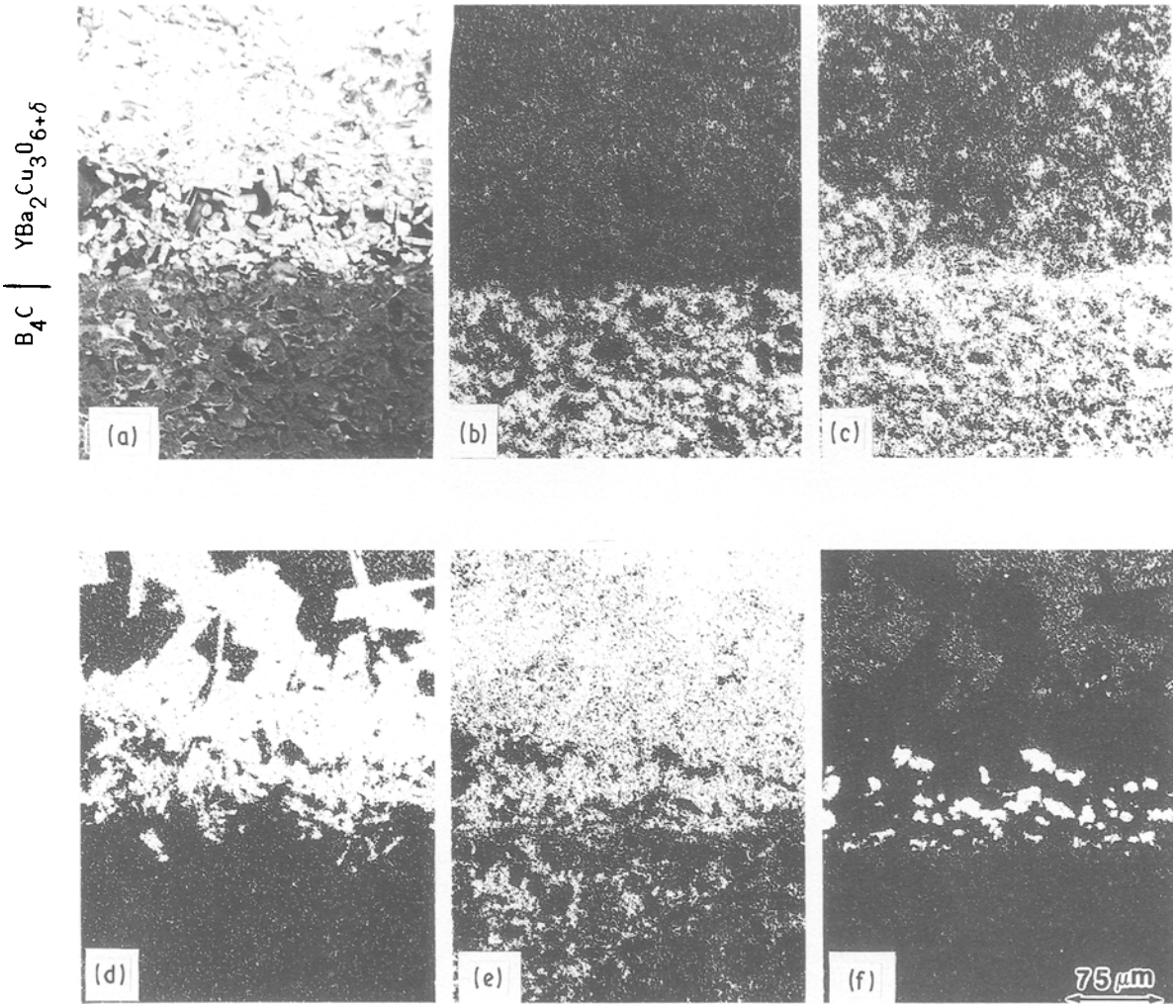

Figure 6 EPMA of the boron carbide–$YBa_2Cu_3O_{6+\delta}$ reaction couple treated at 950 °C for 19 h. (a) Backscattered electron image, and elemental maps for (b) boron, (c) carbon, (d) yttrium, (e) barium, and (f) copper.

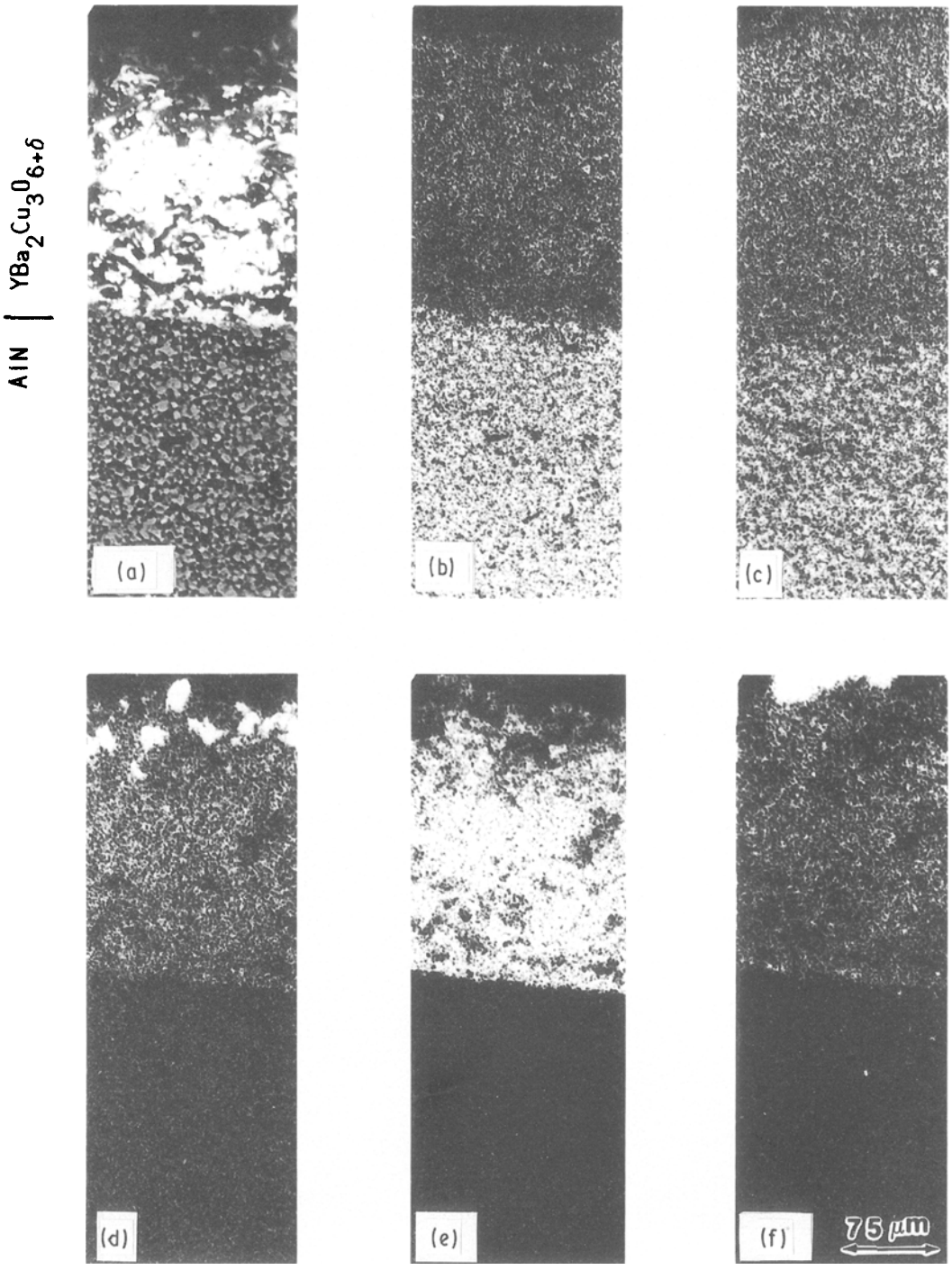

Figure 7 EPMA of the aluminium nitride–$YBa_2Cu_3O_{6+\delta}$ reaction couple treated at 950 °C for 19 h. (a) Backscattered electron image, and elemental maps for (b) aluminium, (c) nitrogen, (d) yttrium, (e) barium, and (f) copper.

reaction and the width of the reaction zone eliminate aluminium nitride from further consideration in processing $YBa_2Cu_3O_{6+\delta}$.

3.7. Boron nitride

The boron nitride–$YBa_2Cu_3O_{6+\delta}$ reaction couple fragmented during the heat treatment, 950 C° for 19 h. This was probably due to water adsorbed in the boron nitride. However, as analysis of fragments of the reaction couple showed metallic copper, no further work was done with this material.

3.8. Boron nitride–titanium diboride composite

When boron nitride was combined with titanium diboride, the reaction couple survived the thermal treatments at both 850 and 950 °C. After 4 h at 850 °C, titanium has diffused into the $YBa_2Cu_3O_{6+\delta}$, see Fig. 8, and there is indication of copper segregation at the interface. Yttrium is clustered unevenly in the $YBa_2Cu_3O_{6+\delta}$ phase, possibly as Y_2BaCuO_5. The width of the reaction interface is evident in Fig. 9, which contains the elemental maps of the reaction couple treated at 950 °C for 19 h. Copper has clearly penetrated into the composite leaving a nearly copper-

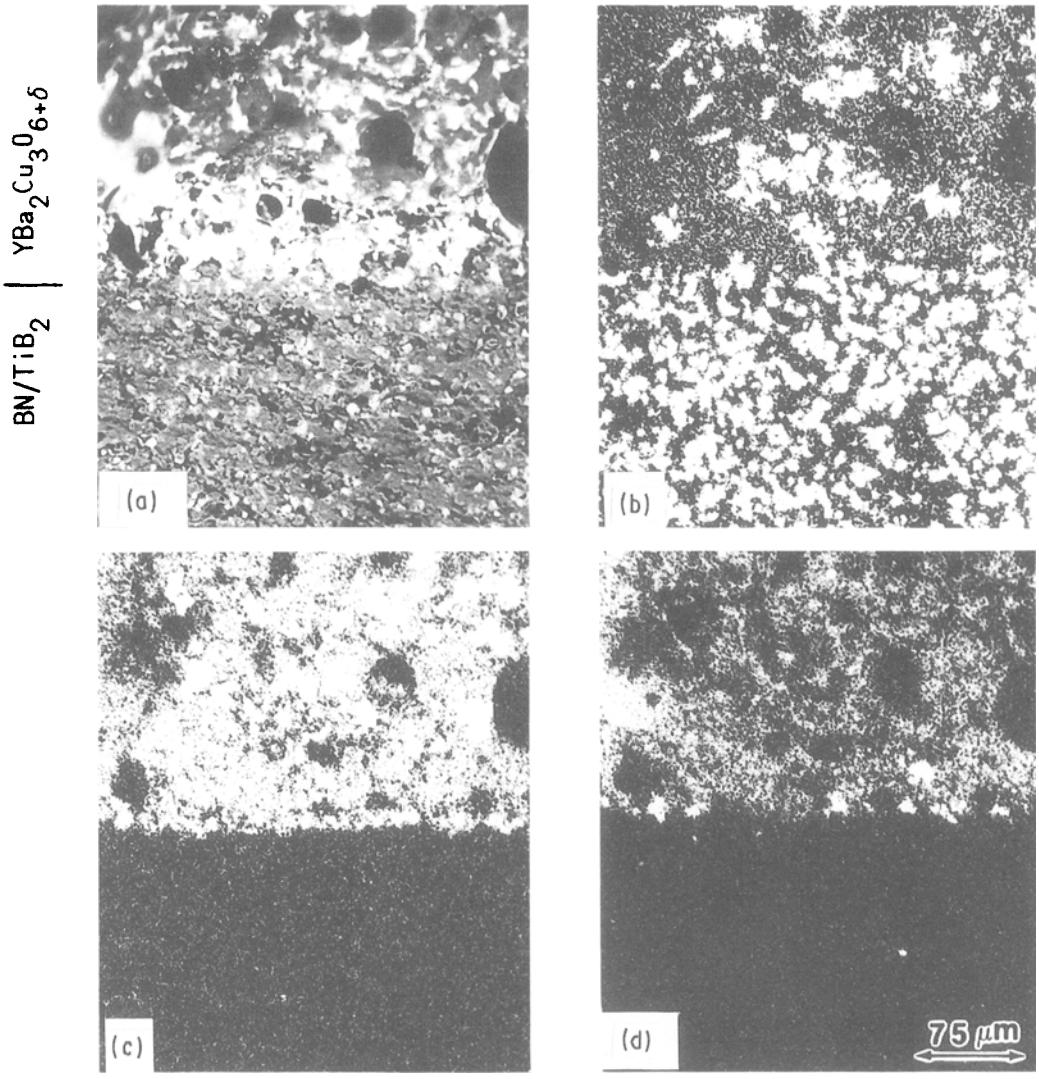

Figure 8 EPMA of the boron nitride–titanium diboride composite–$YBa_2Cu_3O_{6+\delta}$ reaction couple treated at 850 °C for 4 h. (a) Backscattered electron image, and elemental maps for (b) titanium, (c) yttrium, and (d) copper.

free zone in the $YBa_2Cu_3O_{6+\delta}$. Titanium has penetrated throughout the $YBa_2Cu_3O_{6+\delta}$ which, in turn, has undergone grain growth. Acicular grains evident in the yttrium and copper maps, are yttrium-rich and copper-poor. This material is also not suitable for die materials.

3.9. Zirconium diboride

There was no wetting between the two components of the zirconium diboride–$YBa_2Cu_3O_{6+\delta}$ reaction couple when reacted at 850 °C for 4 h. However, some segregation of yttrium, and to a lesser extent, copper, occurred, see Fig. 10. The surface of the zirconium

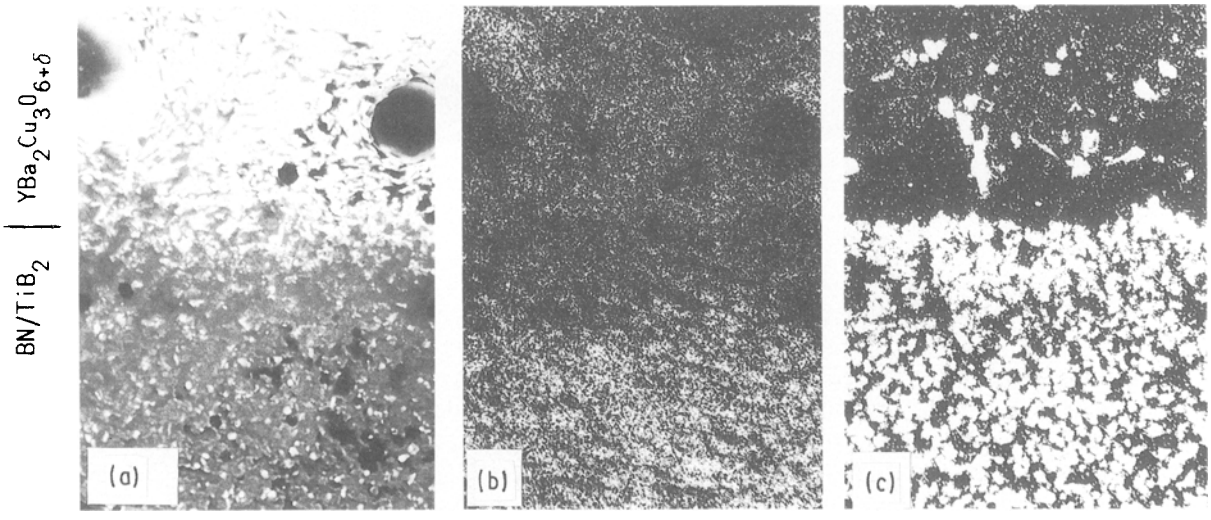

Figure 9 EPMA of the boron nitride–titanium diboride composite–$YBa_2Cu_3O_{6+\delta}$ reaction couple treated at 950 °C for 19 h. (a) Backscattered electron image, and elemental maps for (b) titanium, (c) boron, (d) yttrium, (e) barium, and (f) copper.

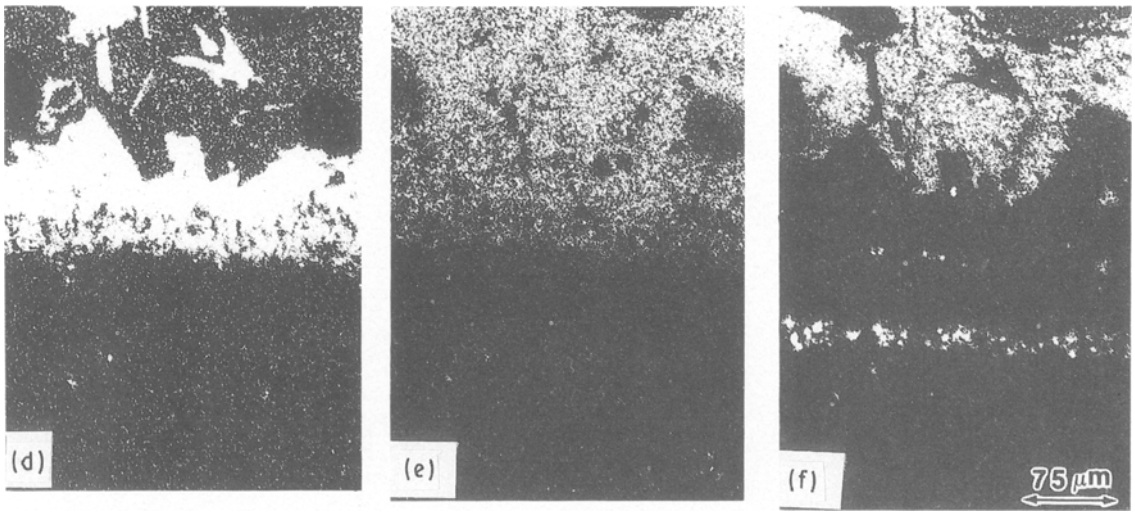

Figure 9 Continued.

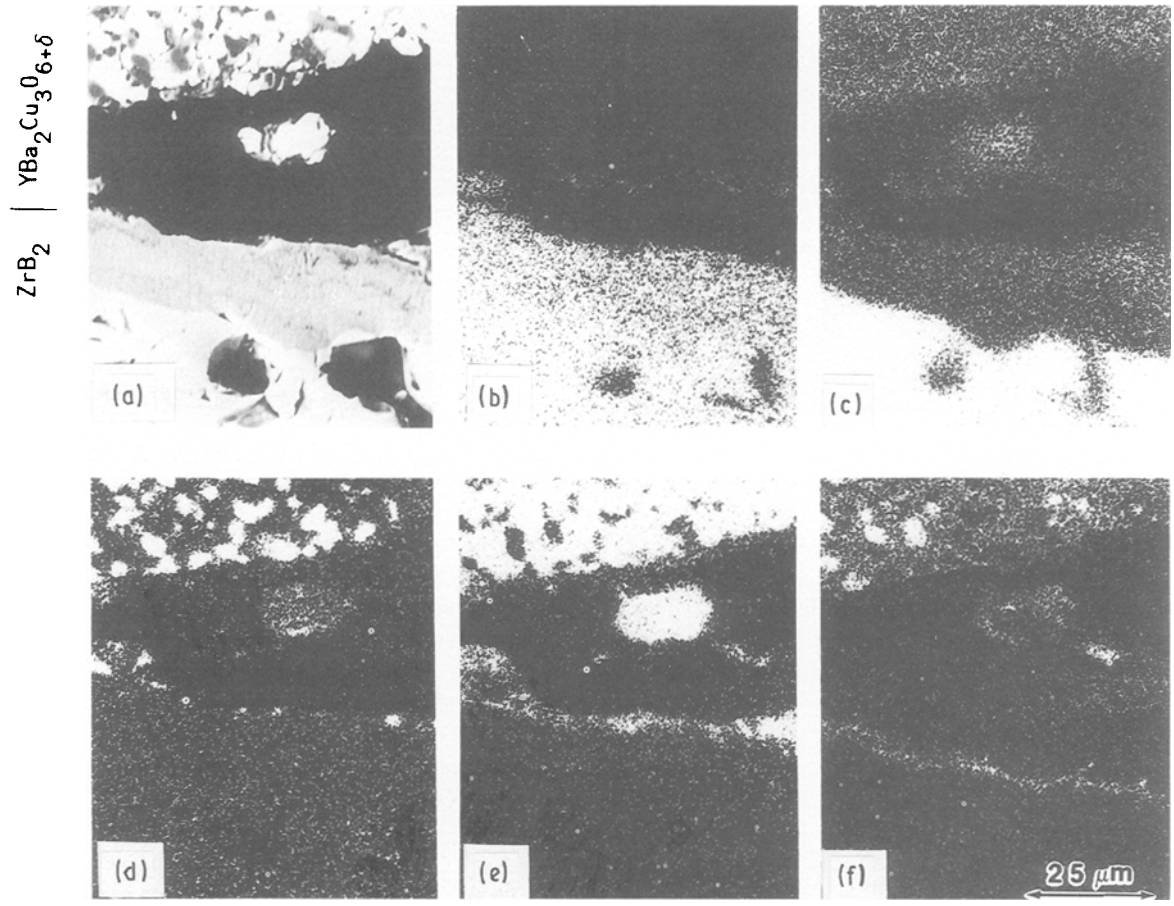

Figure 10 EPMA of the zirconium diboride–$YBa_2Cu_3O_{6+\delta}$ reaction couple treated at 850 °C for 4 h. (a) Backscattered electron image, and elemental maps for (b) zirconium, (c) boron, (d) yttrium, (e) barium, and (f) copper.

diboride also changed. A boron-poor region formed, possibly due to the formation of a zirconium dioxide phase.

The reactions occurring at the more severe thermal treatment, 950 °C for 19 h, are interesting. A low magnification, backscattered electron image, Fig. 11, shows the reaction zone and the two reaction couple materials on either side. The texture of the zirconium diboride in the reaction zone has become more granular and a needle-like phase has formed that grows into the $YBa_2Cu_3O_{6+\delta}$ phase. The needles are yttrium-rich and copper-poor, see Fig. 12. The barium distribution is uniform. Boron has diffused into $YBa_2Cu_3O_{6+\delta}$ and barium has diffused into zirconium diboride. This material is not promising for $YBa_2Cu_3O_{6+\delta}$ processing applications.

3.10. Aluminium oxide

Prior experience with this material in our laboratory has shown that extensive wetting and reaction occur

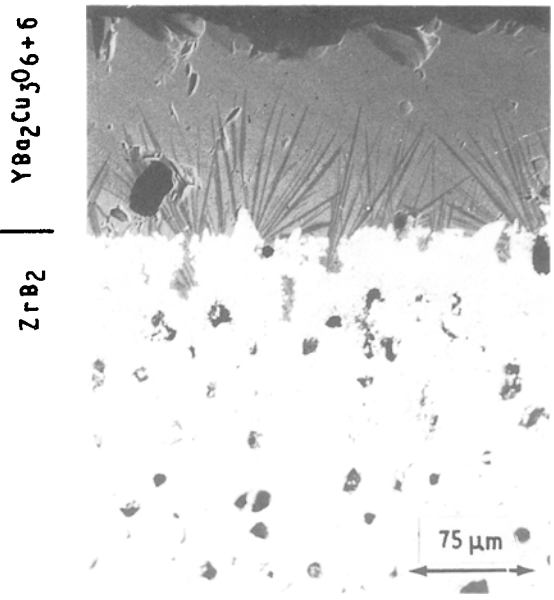

Figure 11 EPMA of the zirconium diboride–$YBa_2Cu_3O_{6+\delta}$ reaction couple treated at 950 °C for 19 h. Backscattered electron image.

when $YBa_2Cu_3O_{6+\delta}$ precursors are reacted in aluminium oxide crucibles. Usually CuO and Y_2BaCuO_5 are detected in the product. The aluminium oxide–$YBa_2Cu_3O_{6+\delta}$ reaction couple was treated at 950 °C for 19 h. As expected, aluminium oxide was wetted by reaction products and a green layer, Y_2BaCuO_5, was observed along the interface.

EPMA maps of the aluminium oxide–$YBa_2Cu_3O_{6+\delta}$ reaction couple are shown in Fig. 13. The interface is sharp with little penetration of barium or copper into the bulk of the aluminium oxide. The level of aluminium ion diffusion into the $YBa_2Cu_3O_{6+\delta}$ is very slight, probably less than 2% concentration based on EPMA results. Aluminium is known to substitute for copper in the $YBa_2Cu_3O_{6+\delta}$ lattice, but has a negligible effect on its critical temperature at this level [10]. The effect of aluminium substitution on critical current has not been determined. Whereas aluminium oxide may continue to be used as a substrate for sintering, provided powders of $YBa_2Cu_3O_{6+\delta}$ are used between the aluminium oxide and the $YBa_2Cu_3O_{6+\delta}$ specimen, the degree of wetting observed does not encourage its use as a hot-pressing or hot-forging material.

4. Conclusion

Eleven ceramic materials were tested for chemical compatibility with $YBa_2Cu_3O_{6+\delta}$. The objective was to identify materials that would not react with $YBa_2Cu_3O_{6+\delta}$ and therefore would be suitable to contain $YBa_2Cu_3O_{6+\delta}$ in hot-forging experiments. Of interest was the degree of wetting between the components of the reaction couple (the ceramic material and $YBa_2Cu_3O_{6+\delta}$), the nature and extent of chemical reaction, and its effect on residual $YBa_2Cu_3O_{6+\delta}$.

Four compounds show promise for use as die materials for studies of hot forging of $YBa_2Cu_3O_{6+\delta}$: barium zirconate, silicon carbide, magnesium oxide, and zirconium dioxide. Barium zirconate and silicon carbide show essentially no wetting or chemical reac-

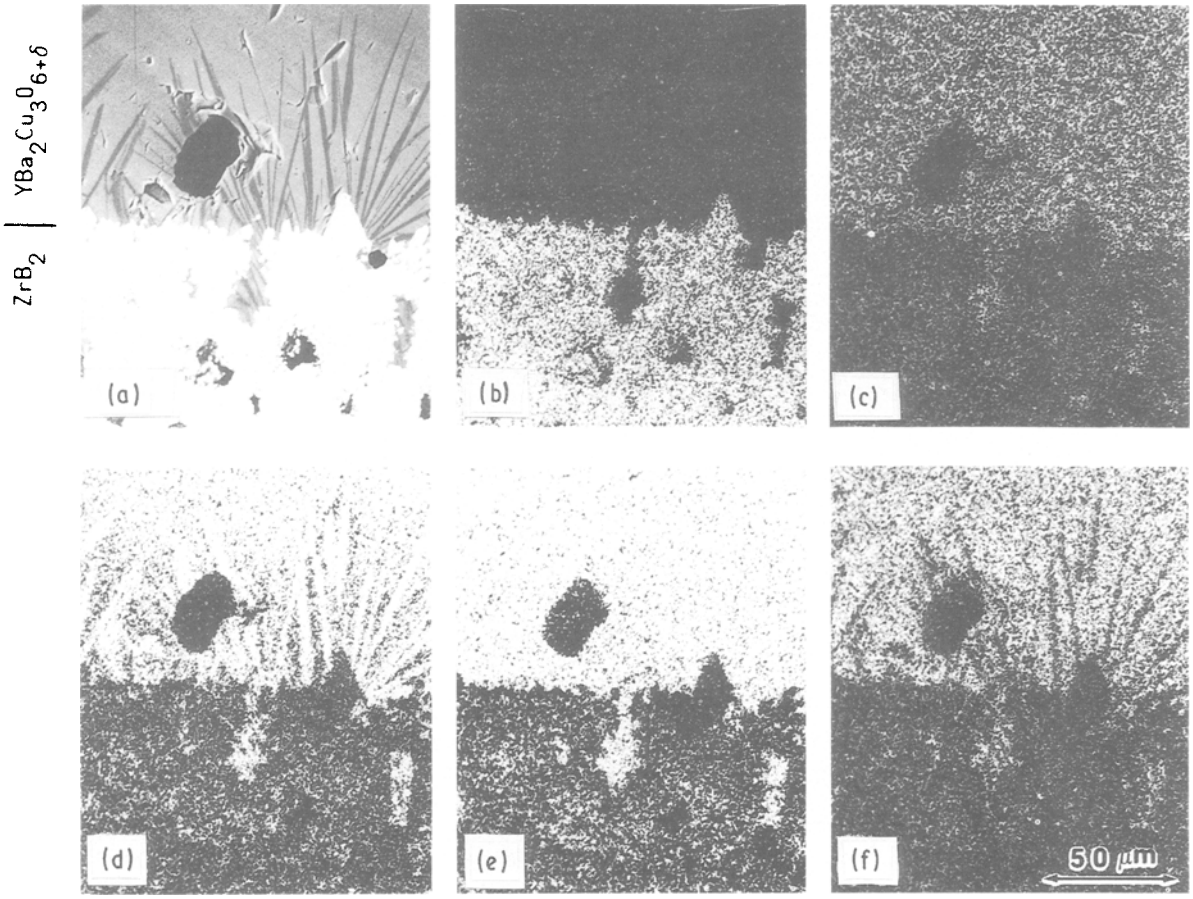

Figure 12 EPMA of the zirconium diboride–$YBa_2Cu_3O_{6+\delta}$ reaction couple treated at 950 °C for 19 h. (a) Backscattered electron image and elemental maps for (b) zironium, (c) boron, (d) yttrium, (e) barium, and (f) copper.

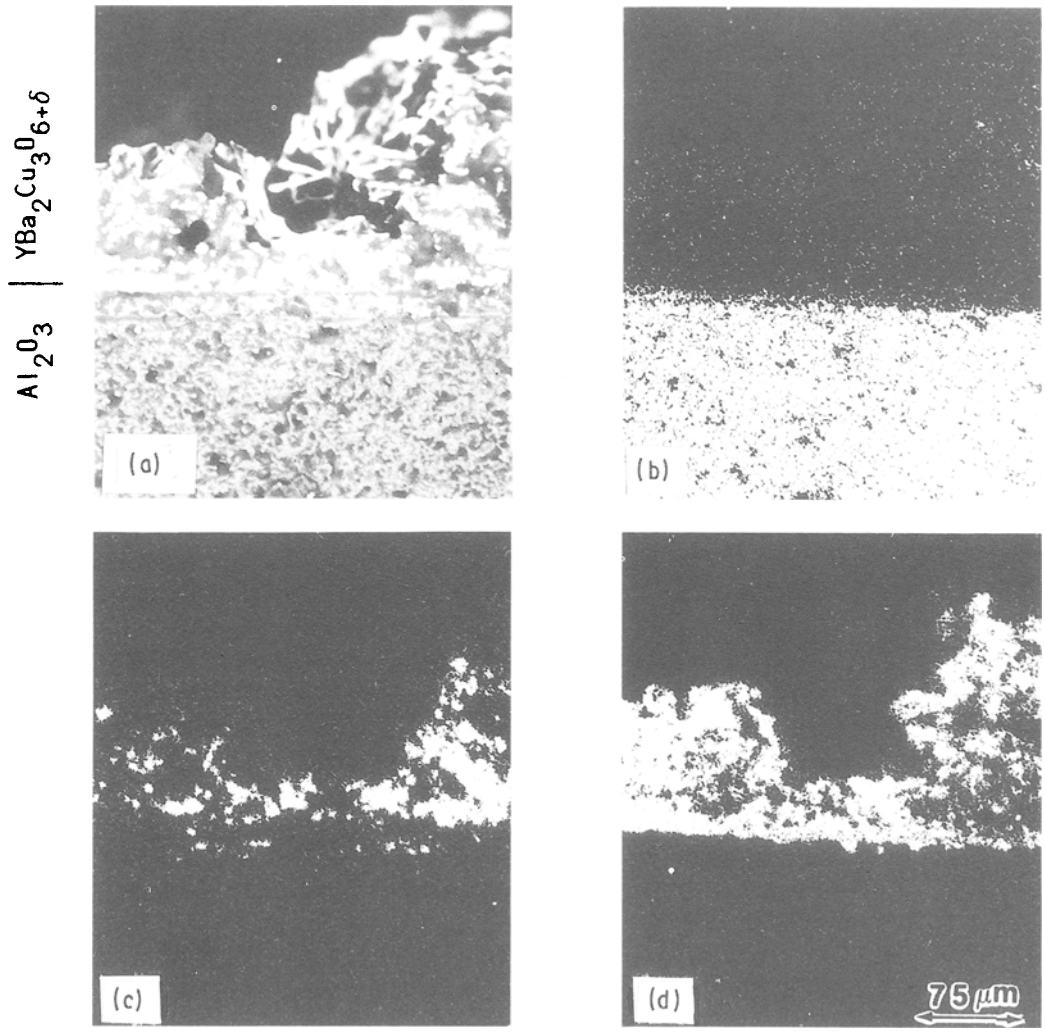

Figure 13 EPMA of the aluminium oxide–$YBa_2Cu_3O_{6+\delta}$ reaction couple treated at 950 °C for 19 h. (a) Backscattered electron image, and elemental maps for (b) aluminium, (c) barium, and (d) copper.

tion with $YBa_2Cu_3O_{6+\delta}$. Magnesium oxide and zirconium dioxide react with $YBa_2Cu_3O_{6+\delta}$, but it appears that each reaction is limited to a very narrow interface. Though not described in detail in this work, it was later shown by the authors that $YBa_2Cu_3O_{6+\delta}$ could, in fact, be hot forged using a zirconium dioxide die and die inserts without adhesion occurring between $YBa_2Cu_3O_{6+\delta}$ and zirconium dioxide.

The remaining compounds studied undergo various reactions with $YBa_2Cu_3O_{6+\delta}$. The nitrides and boron carbide reduce $YBa_2Cu_3O_{6+\delta}$ resulting in the segregation of metallic copper to the carbide or nitride side of the reaction interface. The reaction of $YBa_2Cu_3O_{6+\delta}$ with zirconium diboride results in the formation of yttrium-rich needles that grow into the $YBa_2Cu_3O_{6+\delta}$ phase from the original reaction interface.

Acknowledgements

The authors thank several colleagues in the General Motors Research Laboratories for their assistance throughout the course of this work: Jack Johnson for X-ray diffraction analysis, Carl Fuerst and Alan Druschitz for helpful technical discussions. The critical commentaries of James Chen, Steve Gaarenstroom, Richard Hammer, and Sy Katz are also appreciated.

References

1. M. K. WU, J. R. ASHBURN, C. J. TORNG, P. H. HOR, L. R. MENG, L. GAO, Z. J. HUANG, Y. Q. WANG and C. W. CHU, *Phys. Rev. Lett.* **58** (1987) 908.
2. D. DIMOS, P. CHAUDHARI, J. MANNHART and F. K. LeGOUES, *ibid.* **61** (1988) 219.
3. M. N. RAHMAN, L. C. DeJONGHE and C. MAY-YING, *Adv. Ceram. Mater.* **3** (1988) 393.
4. G. BUSSOD, A. PECHNIK, C. CHU and B. DUNN, *J. Amer. Ceram. Soc.* **72** (1989) 137.
5. M. K. IHM, B. R. POWELL and R. L. BLOINK, *J. Mater. Sci.* **25** (1990) 1664.
6. C. T. CHEUNG and E. RUCKENSTEIN, *J. Mater. Res.* **4** (1989) 1.
7. L. A. TIETZ, B. C. DECOOMAN, C. B. CARTER, D. K. LATHROP, S. E., RUSSEK and R. A. BUHRMAN, in "Proceedings of the Symposium on High-Temperature Superconductors", edited by M. Brodsky, R. C. Dynes, K. Kitazawa and H. L. Tuller (Materials Research Society, Pittsburg, PA, 1988) p. 719.
8. M. GURVITCH and A. T. FIORY, *Appl. Phys. Lett.* **51** (1987) 1027.
9. C. H. CHEN, M. HONG, D. J. WERDER, J. KWO, S. H. LIOU and D. D. BALOW, *Appl. Phys. Lett.* **54** (1989) 1579.
10. T. SIEGRIST, L. F. SCHNEEMEYER, J. V. WASZCZAK, N. P. SINGH, R. L. OPILA, B. BATLOGG, L. W. RUPP and D. W. MURPHY, *Phys. Rev. B* **36** (1987) 8365.

Received 1 October 1990
and accepted 18 March 1991